Cosolvent Effects on Protein Stability

Deepak R. Canchi[1] and Angel E. García[2]

[1]Department of Chemical and Biological Engineering, [2]Department of Physics, Applied Physics and Astronomy and Center for Biotechnology and Inter-Disciplinary Studies, Rensselaer Polytechnic Institute, Troy, New York 12180; email: angel@rpi.edu

Annu. Rev. Phys. Chem. 2013. 64:273–93

First published online as a Review in Advance on January 4, 2013

The *Annual Review of Physical Chemistry* is online at physchem.annualreviews.org

This article's doi: 10.1146/annurev-physchem-040412-110156

Keywords

urea, TMAO, preferential interaction, molecular dynamics simulations, protein folding

Abstract

Proteins are marginally stable, and the folding/unfolding equilibrium of proteins in aqueous solution can easily be altered by the addition of small organic molecules known as cosolvents. Cosolvents that shift the equilibrium toward the unfolded ensemble are termed denaturants, whereas those that favor the folded ensemble are known as protecting osmolytes. Urea is a widely used denaturant in protein folding studies, and the molecular mechanism of its action has been vigorously debated in the literature. Here we review recent experimental as well as computational studies that show an emerging consensus in this problem. Urea has been shown to denature proteins through a direct mechanism, by interacting favorably with the peptide backbone as well as the amino acid side chains. In contrast, the molecular mechanism by which the naturally occurring protecting osmolyte trimethylamine *N*-oxide (TMAO) stabilizes proteins is not clear. Recent studies have established the strong interaction of TMAO with water. Detailed molecular simulations, when used with force fields that incorporate these interactions, can provide insight into this problem. We present the development of a model for TMAO that is consistent with experimental observations and that provides physical insight into the role of cosolvent-cosolvent interaction in determining its preferential interaction with proteins.

1. INTRODUCTION

Proteins are biological macromolecules that carry out a range of essential functions in a cell. Structurally, they are heteropolymers of the 20 naturally occurring α-amino acids. The sequence in which the amino acids are joined together, by the peptide bond, defines the primary structure of the protein. Most proteins adopt a well-defined, three-dimensional structure in solution, called the folded or native state, which is essential to enable their biological functions (**Figure 1**). Anfinsen (1)

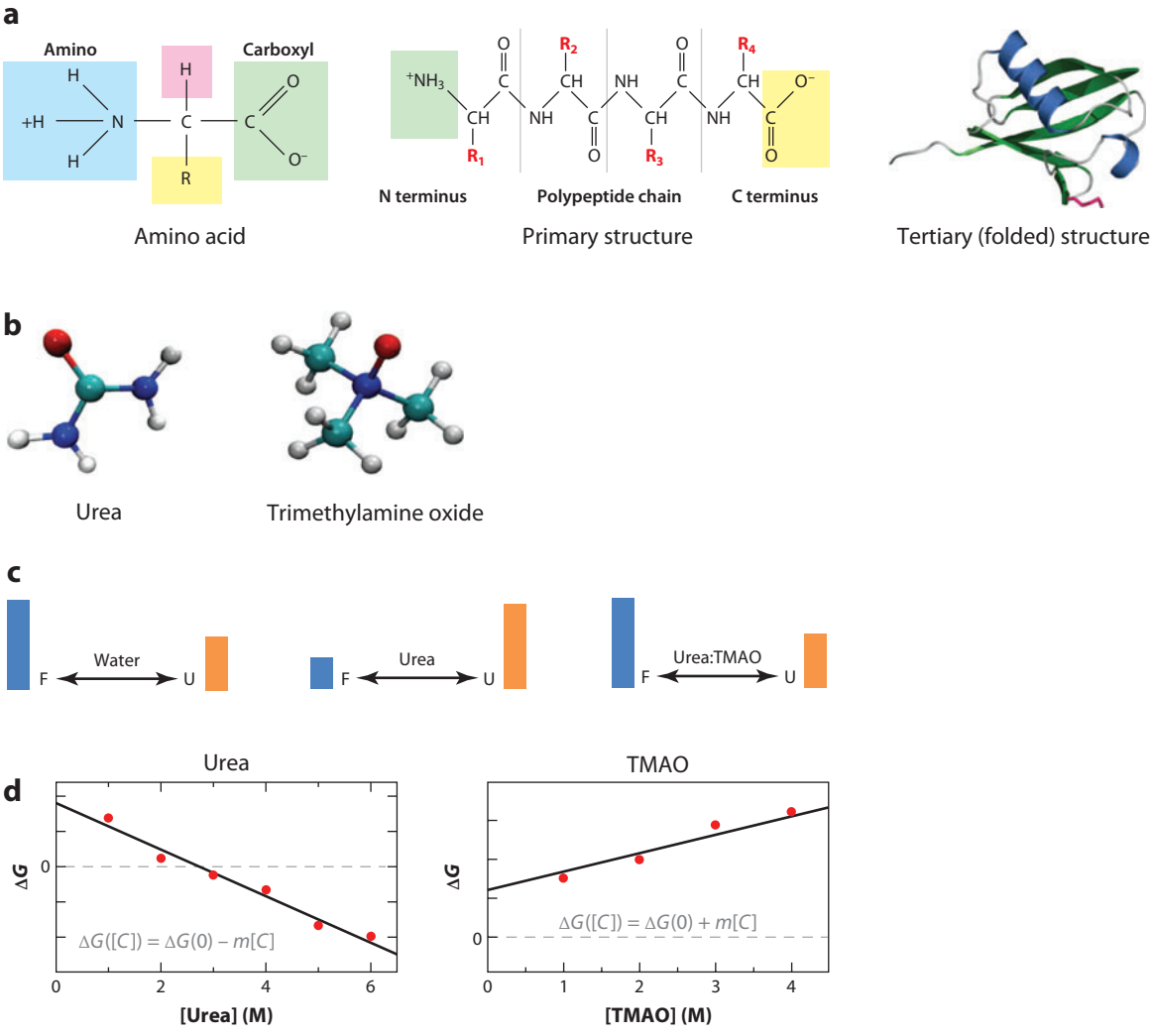

Figure 1

Protein structure, folding equilibrium, and cosolvents. (*a*) Levels of protein structure. The repeating unit -C-O-N-C_α- makes up the backbone of the protein, and R_i represent the various side chains. (*b*) Molecular structure of urea (denaturant) and TMAO (protecting osmolyte). Carbon is shown in cyan, nitrogen in blue, oxygen in red, and hydrogen in white. (*c*) The folding equilibrium of the protein in water is shifted toward the unfolded (U) ensemble in urea. The addition of urea and TMAO in a concentration ratio of 2:1 leaves the folding (F) equilibrium unaffected. (*d*) The free energy of protein unfolding depends linearly on the concentration of the cosolvent. The slope of the fit is known as the *m*-value.

demonstrated that all the information required for a protein to fold to its native state is determined by its amino acid sequence. Proteins fold to a native structure and on short timescales (typically milliseconds), despite having a vast conformational space available to them. This is explained by invoking a funnel-like free energy landscape for the protein in which the folded state lies at the minimum and by noting that the sequences of naturally occurring proteins are minimally frustrated as opposed to random heteropolymers (2, 3).

A protein in solution exists in conformational equilibrium with an ensemble of unfolded states, with the folded ensemble being favored at ambient conditions (**Figure 1**). The equilibrium between the folded and the unfolded ensembles can be perturbed by changing the thermodynamic state of the system (temperature, pressure, pH) or by changing the composition by the addition of cosolvents to the solution (4–7). The process of shifting the conformational equilibrium toward the unfolded ensemble is known as denaturation. Denaturation is an important process in biochemical studies as thermodynamic functions, such as the free energy, enthalpy, and entropy, which provide information about the stability of the folded state, can be obtained only by perturbing the equilibrium to populate the unfolded (denatured) states (4). The population in different ensembles can be obtained by monitoring quantities such as spectral properties, heat capacity, and enzyme activity, from which the equilibrium constant and other thermodynamics quantities can be derived. Many proteins undergo a sharp, cooperative transition from the native to the denatured state upon an increase in temperature, leading to the characteristic sigmoidal curve for the experimental observable (4). Such transitions are treated in a two-state model, with the validity of the assumption judged by comparing the van't Hoff enthalpy with the enthalpy measured by calorimetry.

Proteins are also, counterintuitively, denatured by increasing the pressure and unfold with a decrease in partial molar volume (6, 8–10). It turns out that the packing of the folded state is not optimal, and the volume of the water-swollen unfolded state is smaller than the folded state owing to the hydration of the interior hydrophobic residues (11–13). Phase diagrams for the pressure-temperature behavior of the folding-unfolding transition of proteins have been obtained, from experiments as well as molecular simulations (14–18), providing a unified thermodynamic description for pressure, heat, and cold denaturation.

In this review, we describe how the addition of small organic molecules, known as cosolvents, affects the folding equilibrium of proteins (7). These molecules are termed cosolvents as they occupy a significant fraction of the solution volume. Remarkably, the equilibrium can be favored in either direction, depending on the identity of the cosolvent (**Figure 1*b*,*c***). Cosolvents such as urea and guanidinium chloride that favor the unfolded states are known as denaturants. Conversely, compounds such as trimethylamine *N*-oxide (TMAO), glycine, betaine, glycerol, and sugars stabilize the folded state of proteins and are known as protecting osmolytes (7, 19–21). Intriguingly, TMAO can counteract the denaturing effect of urea on proteins, typically in a 2:1 concentration ratio of urea and TMAO (19, 22). We focus on the effects of urea and TMAO on protein stability and show how an interplay of molecular dynamics (MD) simulations and experiments can prove successful in uncovering the molecular basis of these phenomena.

Cosolvent: small, neutral organic molecules that can modulate protein stability

van't Hoff enthalpy: enthalpy obtained by analysis of the temperature dependence of the equilibrium constant

TMAO: trimethylamine *N*-oxide

Molecular dynamics (MD): computational technique to study the microscopic motions of atoms and molecules; molecular trajectories are obtained by numerically integrating Newton's equations of motion

Linear extrapolation model (LEM): used to model the dependence of protein stability on cosolvent concentration

2. PROTEIN DENATURATION BY UREA

The ability of urea to denature proteins has been long known (23) and is used ubiquitously in protein folding studies. Experimentally, it is observed that the free energy of protein unfolding decreases linearly with urea concentration. This observation is widely used to estimate the stability of proteins in water via the linear extrapolation model (LEM); i.e., $\Delta G^{Urea} = \Delta G^{Water} - m[C]$ (24, 25) (**Figure 1*d***). The slope of the linear fit, known as the *m*-value, is a measure of the response

of protein stability to the addition of urea. It is of interest to understand the molecular mechanism by which urea denatures proteins, given its importance in protein folding. This question has attracted much debate over the past 50 years, the challenge being that protein-urea interactions are weak and large concentrations are required to denature proteins.

Hydrophobic effect: the tendency of nonpolar molecules to aggregate in aqueous solution and exclude water

Dispersion interaction: weak, attractive noncovalent interaction between electrically neutral molecules, which includes dipole-dipole, dipole-induced dipole, and London forces

2.1. Suggested Mechanisms

There are two basic schools of thought in explaining the denaturing effect of urea on proteins. The indirect mechanism postulates that urea causes the denaturation of proteins by the alteration of water structure, a view that emerged from transfer experiments showing that hydrocarbons are more soluble in aqueous urea than water (26). The implication here is that the addition of urea alters the structure of water to enable the ready solvation of alkanes by weakening the hydrophobic effect, which is a major driving force for protein folding (27). This view has been questioned by recent experimental and computational studies demonstrating that urea integrates well into the hydrogen-bonding network of water without affecting water's spatial distribution around itself, while showing a minimal tendency for self-aggregation (28–34). To our knowledge, there have been no experimental studies that provide convincing evidence linking the denaturing effect of urea to its effect on water structure.

Conversely, we have the direct mechanism, in which urea denatures proteins owing to its local interaction with the protein, rather than owing to differences in the global properties of aqueous urea over water. Proteins are chemically heterogeneous, consisting of the peptide backbone and amino acid side chains, which can be polar, apolar, or charged. Within the direct mechanism model, the nature and strength of urea's interactions with the various protein moeities have been extensively studied. An enduring explanation for this phenomenon has been that urea unfolds proteins by forming hydrogen bonds with the protein backbone (21, 35). The attractiveness of this idea is easy to see: Urea is chemically similar to the peptide backbone, and it is believed that urea competes with the intrabackbone hydrogen bonds that stabilize protein secondary structure motifs, such as α-helices and β-sheets, to cause protein unfolding. However, urea can also have favorable interaction with the various amino acid side chains in the protein (34, 36–38). Quantifying the interactions of urea with individual amino acids and the contribution of these interactions to the overall thermodynamics of the phenomenon will provide a clear picture of the molecular basis of chemical denaturation. MD simulations have been used to examine the nature of protein-urea interactions, i.e., by studying the contribution of electrostatic and dispersion interactions to the energetics of unfolding to provide insight into the groups interacting with urea. If the hydrogen bonding of urea to the peptide backbone drives unfolding, then the electrostatic interactions must be dominant. On the contrary, the dominance of dispersion interactions points to a weak nonspecific interaction of urea with the entire protein surface, including the apolar groups.

Examining the process from a thermodynamic viewpoint by studying the enthalpy-entropy contributions to the free energy can help distinguish between the indirect and direct mechanisms. The free energy of unfolding decreases linearly with urea concentration (24, 25), and an enthalpic origin of this behavior is indicative of the direct mechanism. If the entropic contribution dominates, then nonlocal effects such as entropic gain due to the displacement of water by larger urea molecules must be accounted for (39). An aspect that has not received much attention is the study of the thermodynamics of urea denaturation as a function of temperature and pressure (13). Urea is used in high-pressure denaturation experiments to lower the pressure at which the protein unfolds, but it is not clear if the different modes of protein denaturation are additive or interact in a synergistic manner.

2.2. Insights from Molecular Dynamics Simulations

Urea denaturation has been extensively studied using MD simulations of both model systems and proteins. Model systems are chosen such that the effects of charge and polarity can be separated from purely hydrophobic effects. Studies of small hydrophobic solutes in urea solutions have led to conflicting results regarding the weakening of the hydrophobic effect owing to the addition of urea (40–44). However, the effect of urea has been clearly observed in simulations of model hydrophobic systems at a larger length scale. England et al. (45) showed that the attraction between hydrophobic plates is reduced in urea because of the stabilization of the liquid phase between the plates against dewetting. A purely hydrophobic polymer was shown to unfold in urea owing to the formation of enthalpically favorable dispersion interactions of the denaturant with the polymer (46). Similarly, it has been found that urea accumulates around and in the interior of carbon nanotubes (47, 48). These studies show that urea can modulate the hydrophobic effect by making energetically favorable contacts with the purely hydrophobic groups. Urea has also been found to interact favorably with charged solutes through hydrogen bonding and to disrupt ion pairs (40, 44).

Force field: specifies the functional form and the numerical parameters for interaction among molecules in an MD simulation

Most reported simulation studies of proteins in aqueous urea have sought to understand the phenomenon in a mechanistic manner, i.e., unfold the protein starting from the native state and calculate observables based on a few simulation trajectories (33, 44, 49–53). Some studies attributed the denaturation to both direct and indirect mechanisms (50, 51), whereas others emphasized the role of hydrogen bonding between urea and the protein backbone (44, 54, 55). Simulations of individual amino acids in aqueous urea have shown that urea has a favorable interaction with almost all amino acids, leading to its preferential binding to amino acids over water (34, 36). Large-scale simulations of lysozyme in urea demonstrated the importance of urea's dispersion interactions in facilitating protein unfolding (33). The aforementioned simulation studies provided valuable insight into various modes of urea's interaction with proteins, especially by highlighting the role of protein-urea dispersion interactions. However, these studies do not address the balance of the driving forces for denaturation, which can be obtained only from simulations of the protein folding equilibrium in the presence of urea (56, 57).

The choice of the force fields used to model the solvent environment needs particular attention. To simulate cosolvent effects on protein stability using MD, one must address the balance of interactions among the various species in solution. It is necessary that the force fields employed adequately reproduce solution thermodynamic data for the cosolvent-water system before the interaction with the protein is considered. Solution thermodynamic data such as partial molar volumes, activity coefficients, and osmotic coefficients are reflections of the solute-solute, solute-solvent, and solvent-solvent interactions in the solution. Smith and coworkers (58–61) have pioneered the parameterizing of solute/cosolvents to reproduce bulk solution thermodynamic properties using the Kirkwood-Buff (KB) theory for solutions, a statistical mechanical theory for multicomponent solutions that relates the integrals of pair correlation functions of the species to bulk thermodynamic measurements (62, 63). The KBFF model (58), which is the model for urea developed using the KB theory, and the OPLS model (64) are commonly used for simulations of urea-water mixtures. In an insightful study, Horinek & Netz (34) showed that unlike the KBFF model, the OPLS model displays strong urea-urea attraction, leading to a deviation from experimental activity data. The nonideality in the OPLS model results in erroneous contributions from direct and indirect effects when considering the interaction of urea with peptides and proteins, whereas the indirect contribution in the KBFF model is negligible. In the following sections, we introduce experimental methods and models used to study and interpret the effect of urea (and other cosolvents) on protein stability before bridging computational and experimental results.

2.3. Transfer Model

Förster resonance energy transfer (FRET): provides a measurement of the distance between two fluorophores

Small-angle X-ray scattering: provides information about the shape and size of macromolecules

Equilibrium dialysis: technique to study the interaction of cosolvents with a macromolecule by measuring the cosolvent concentration in two solutions separated by a semipermeable membrane that does not allow the macromolecule to pass

Osmometry: technique to determine protein-cosolvent interaction by measuring changes in vapor pressure of the water owing to the addition of protein and/or cosolvent

One popular model to study the influence of cosolvents on protein stability is the transfer model proposed by Tanford (65). In this model, the folding/unfolding of the protein and the process of the transfer of folded and unfolded states from water to aqueous urea solution are tied together in a thermodynamic cycle. According to the transfer model, the free energy of protein unfolding in a 1-*M* urea solution (ΔG_{1M}^{Urea}) is related to the free energy of unfolding in water (ΔG^{Water}) through

$$\Delta G_{1M}^{Urea} = \Delta G^{Water} + \sum_i n_i \alpha_i \delta g_i^{tr}. \quad (1)$$

Here α_i is the fractional change in the solvent-accessible surface area of group *i* upon unfolding, δg_i^{tr} is the experimentally measured free energy of transfer of group *i* from water to a 1-*M* urea solution, and n_i is the number of groups of type *i* present in the protein (22, 35). In this model, it is assumed that the interaction of various groups with urea contributes in an additive manner to unfolding. Solubility measurements are used to determine δg^{tr} for amino acids and model compounds (22), and the exposed surface area in the unfolded ensemble, and thereby α_i, is determined using polymer models (35).

The contribution of each side-chain group is obtained by subtracting the δg^{tr} of glycine from the δg^{tr} of the corresponding amino acid. The transfer model can be related to the *m*-value by invoking the LEM; i.e., $\sum_i n_i \alpha_i \delta g_i^{tr} = -m$. Using this approach, Bolen and coworkers (21, 35, 66) successfully predicted *m*-values for a large number of proteins. Decomposing the *m*-value into group contributions, they suggested that the dominant contribution to the free energy of unfolding in urea arises from favorable interactions of urea with the peptide backbone, and the total contribution of the interactions between urea and the side chains may even be unfavorable. The application of this model to protecting osmolytes suggested that the increased stability of proteins in osmolytes results from unfavorable backbone-osmolyte interactions (21).

Single-molecule Förster resonance energy transfer (FRET) experiments as well as simulations have shown that the conformations in the denatured ensemble expose more surface area as the concentration of the denaturant increases (56, 67–69). The transfer model, as described above, assumes an unfolded ensemble that is independent of denaturant concentration. Haran and colleagues (70, 71) proposed a modification to the transfer model in which folding is preceded by a coil–to–molten globule collapse transition and were able to demonstrate that denaturants modulate folding by affecting the collapse transition of proteins. In this model, the free energy of collapse from a denatured state to a collapsed state has a linear dependence on denaturant concentration, with the slope similar to the *m*-value from LEM analysis. However, the dependence of the unfolded ensemble on denaturant concentration has not been fully accepted because of disagreement between FRET and small-angle X-ray scattering data, in which no dependence of the scattering profile on the denaturant is observed (72).

2.4. Preferential Interaction Coefficients

The interaction of cosolvents with proteins or other biomolecules can be quantified by measuring the preferential interaction coefficient, defined as

$$\Gamma = -\left(\frac{\partial \mu_2}{\partial \mu_3}\right)_{m_2,T,P} = \left(\frac{\partial m_3}{\partial m_2}\right)_{\mu_3,T,P}, \quad (2)$$

where μ is the chemical potential, *m* is the concentration, and the subscripts 1, 2, and 3 indicate water, the protein, and the cosolvent, respectively (73). Preferential interaction is measured using either equilibrium dialysis (74) or, more recently, vapor pressure osmometry (20). It represents

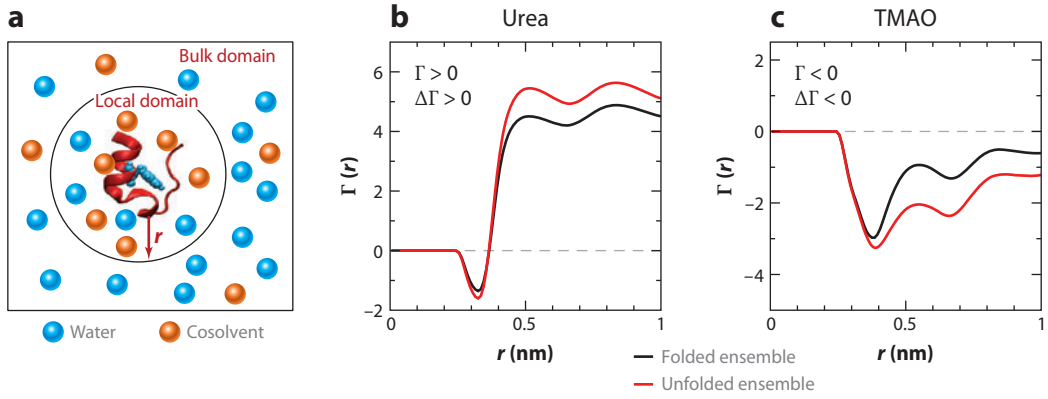

Figure 2

Preferential interaction, denaturants and osmolytes. (*a*) Schematic illustrating the interaction of a protein with water and a cosolvent. The preferential interaction is calculated from molecular dynamics simulations using $\Gamma = \langle N_{cs}^{local} - (\frac{N_{cs}^{bulk}}{N_{w}^{bulk}}) N_{w}^{local} \rangle$, where N_{cs} and N_w denote the number of cosolvent and water molecules, respectively. The quantity is calculated as a function of the boundary of the local domain of the protein, *r*. (*b*) The preferential interaction of a protein with urea. Both Γ and $\Delta\Gamma = \Gamma^{Unfold} - \Gamma^{Fold}$ are positive, signifying the accumulation of urea in the local domain of the protein. (*c*) The preferential interaction of a protein with TMAO. Both Γ and ΔΓ are negative, signifying the exclusion of TMAO from the local domain of the protein.

the change in the chemical potential of a protein in response to the addition of a cosolvent and can also be expressed as the change in the cosolvent concentration to maintain constant chemical potential when a protein is added to the solution. This has been interpreted using a two-domain model as the difference in the cosolvent concentration in the local domain of the protein and the bulk solution (75, 76); i.e.,

$$\Gamma = \left\langle N_3^{local} - \left(\frac{N_3^{bulk}}{N_1^{bulk}} \right) N_1^{local} \right\rangle, \tag{3}$$

where *N* denotes the number of molecules (**Figure 2**). Denaturants such as urea show a positive value of Γ, implying an accumulation of the cosolvent in the vicinity of the protein owing to a net favorable interaction. Conversely, protecting osmolytes show negative values of Γ; i.e., they are excluded from the local domain of the protein because of net unfavorable interactions with the protein surface (7). The above expression lends itself to the calculation of the preferential interaction directly from all-atom MD simulations (77). The preferential interaction is calculated as a function of the distance from the protein surface, and a suitable cutoff distance is applied to determine the value of Γ.

The difference in the preferential interaction of the cosolvent with the protein in its unfolded and folded states can be related to the free energy of protein unfolding in the presence of the cosolvent using the Wyman linkage relation (73),

$$\left(\frac{\partial \ln K}{\partial \ln a_3} \right)_{m_2} = \Delta\Gamma = \Gamma^{Unfold} - \Gamma^{Fold}. \tag{4}$$

Here *K* is the equilibrium constant for the folding reaction $Fold \rightleftharpoons Unfold$, and a_3 is the activity of the cosolvent. Simplifying the above expression by using the LEM for the free energy of unfolding (**Figure 1*d***), we obtain a relation between the *m*-value and preferential interaction,

$$m = RT \frac{|\Delta\Gamma|}{[C]}, \tag{5}$$

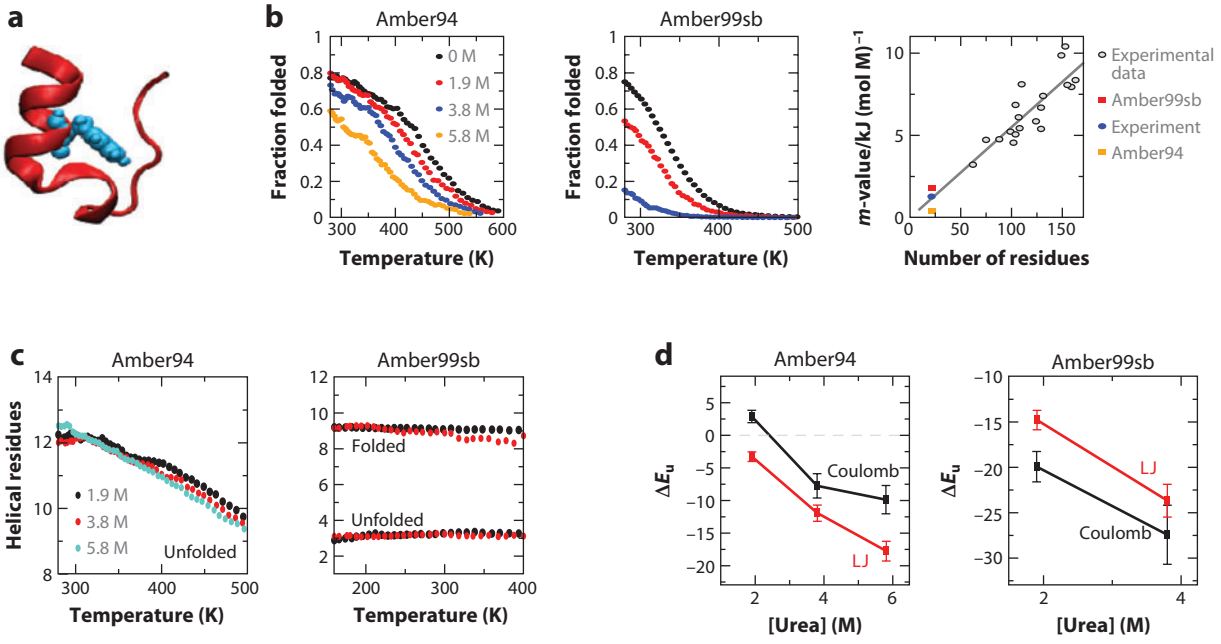

Figure 3

Folding equilibrium of the Trp-cage miniprotein in urea using replica exchange molecular dynamics (56, 57). (*a*) Structure of the 20-residue Trp-cage miniprotein. Tryptophan is shown in cyan. (*b*) Melting curves of Trp-cage in various concentrations of urea, shown for the Amber94 and Amber99sb models. The *m*-values obtained from the simulations agree well with the experimental measurement for Trp-cage, shown along with experimental *m*-values for larger globular proteins. Panel *b* adapted with permission from Reference 56. Copyright 2010, American Chemical Society. (*c*) The average number of helical residues in protein as a function of temperature. Unlike the Amber99sb model, the unfolded ensemble in Amber94 shows significant helical content. (*d*) Change in protein-urea interaction energy upon unfolding. For both the models, the Lennard-Jones (LJ) interaction makes a significant contribution to the total change. Panels *c* and *d* adapted with permission from Reference 57. Copyright 2011, Elsevier.

where $[C]$ is the molar concentration of the cosolvent. This expression provides a molecular interpretation for the *m*-value in terms of the equilibrium distribution of the cosolvent around the protein. $\Delta\Gamma$ is positive for denaturants, implying a greater preferential interaction between the protein and the cosolvent in the unfolded ensemble. Alternatively, osmolytes are expected to be excluded more from the unfolded ensemble than the folded ensemble, and therefore $\Delta\Gamma$ is negative (**Figure 2**). In the analysis of molecular simulation data, although many quantities, such as the number of protein-cosolvent hydrogen bonds and changes in the exposed surface area, provide structural insight into the problem, we stress that calculation of the preferential interaction provides the natural metric for deducing the thermodynamics of the system considered.

Replica exchange molecular dynamics (REMD): an algorithm used to enhance the sampling rugged energy landscapes of complex systems such as protein folding

2.5. Emerging View of Urea Denaturation

Recent computational and experimental studies indicate a converging opinion on the role of various interactions that govern protein denaturation in urea. Canchi and coworkers (56, 57) reported extensive all-atom replica exchange MD (REMD) simulations to obtain the folding equilibrium of the Trp-cage miniprotein in the presence of urea, over a wide range of urea concentrations. Trp-cage, a designed 20-residue protein with a nontrivial fold (78) (**Figure 3*a***), is a system with

a wealth of experimental data available (79–82). The folding of Trp-cage can be described by a two-state model and shows thermodynamic features observed for globular proteins (83). Two different force fields for the protein—Amber94 (84) and Amber99sb (85)—that differ only in the backbone torsion angle potential were employed to study the dependence of the computed driving forces on the unfolded ensemble sampled. The KBFF urea model (58), discussed above, and the TIP3P water model (86) were used to model the solvent. **Figure 3*b*** shows the melting curves obtained from independent REMD simulations at different urea concentrations. From these simulations, the authors were able to obtain *m*-values in good agreement with the experimental value for Trp-cage (82). Fitting the data globally to a thermodynamic model that accounts for urea concentration, they showed that denaturation was driven by enthalpy, with a weak dependence of entropy on urea concentration (56). The two protein models differ significantly in the unfolded ensemble sampled in the simulations. **Figure 3*c*** shows that substantial helical content persists in the unfolded ensemble obtained in the Amber94 simulations owing to inherent bias in the model. However, the Amber99sb model shows a two-state separation in helical content between folded and unfolded ensembles. Sampling the folding equilibrium permits a detailed comparison of the interaction of urea with both the folded and the unfolded ensembles from which the microscopic driving forces for the phenomenon can be inferred. **Figure 3*d*** shows $\Delta E = E^{Unfold} - E^{Fold}$, where E is the interaction energy of the protein with urea molecules in its local domain. Negative values of ΔE demonstrate that both coulomb and the Lennard-Jones (LJ) interactions of urea with the protein favor unfolding. Although the coulomb interaction is larger in magnitude than the LJ interaction, the LJ interaction makes a significant contribution to the difference between the unfolded and the folded ensembles. Along with the finding that the change in the number of backbone-urea hydrogen bonds upon unfolding was small, these results imply that denaturation cannot be explained solely by the hydrogen bonding of urea to the protein.

Lennard-Jones (LJ) potential: an isotropic 6-12 potential that models strong repulsion among molecules at short distances (Pauli repulsion) and weak attraction at larger distances (van der Waals interaction)

To address the contribution of backbone and side-chain groups to the free energy of unfolding, Canchi & García (57) calculated the change in the preferential interaction of urea with Trp-cage upon unfolding. Urea has a larger preferential interaction with the unfolded ensemble than with the folded ensemble, i.e., $\Delta\Gamma = \Gamma^{Unfold} - \Gamma^{Fold} > 0$, which provides the thermodynamic force for unfolding. The *m*-values derived from $\Delta\Gamma$ using Equation 5 were in good agreement with *m*-values from the LEM analysis, showing thermodynamic consistency in the simulations. The *m*-value has been shown to be proportional to the change in exposed surface area upon unfolding (87), a feature also observed in the above simulations. The change in solvent-accessible surface area in the Amber94 model is smaller compared with that in Amber99sb owing to higher helical content, which results in a smaller *m*-value for Amber94. The simulations also make a thermodynamic argument for the dependence of the unfolded ensemble on urea concentration (70, 71). $\Delta\Gamma^P$ was observed to increase with urea concentration, which is necessary as $m = RT\,\Delta\Gamma/[C]$ is a constant. This is physically feasible only if the unfolded ensemble expands with urea concentration.

The preferential interaction calculated for the protein (Γ^P and $\Delta\Gamma^P$) can be decomposed into backbone and side-chain group contributions, in an additive manner, using the proximity criterion (88) (**Figure 4*a***). The repeating unit of -C-O-N-C_α- was grouped as the backbone, and the remaining protein atoms were classified as side chains. The inherent helical bias in the Amber94 model leads to the sampling of conformations in which the backbone is not fully exposed. In this case, the backbone made no contribution to the increase in the preferential interaction upon unfolding (**Figure 4*b***). This is a remarkable scenario: It shows that the change in the preferential interaction of urea and the side chains upon unfolding was sufficient to capture the experimental thermodynamics (*m*-value) in the Amber94 model. For the more realistic Amber99sb model in which the helical bias is eliminated, the side chains, put together, contribute 60% to the *m*-value

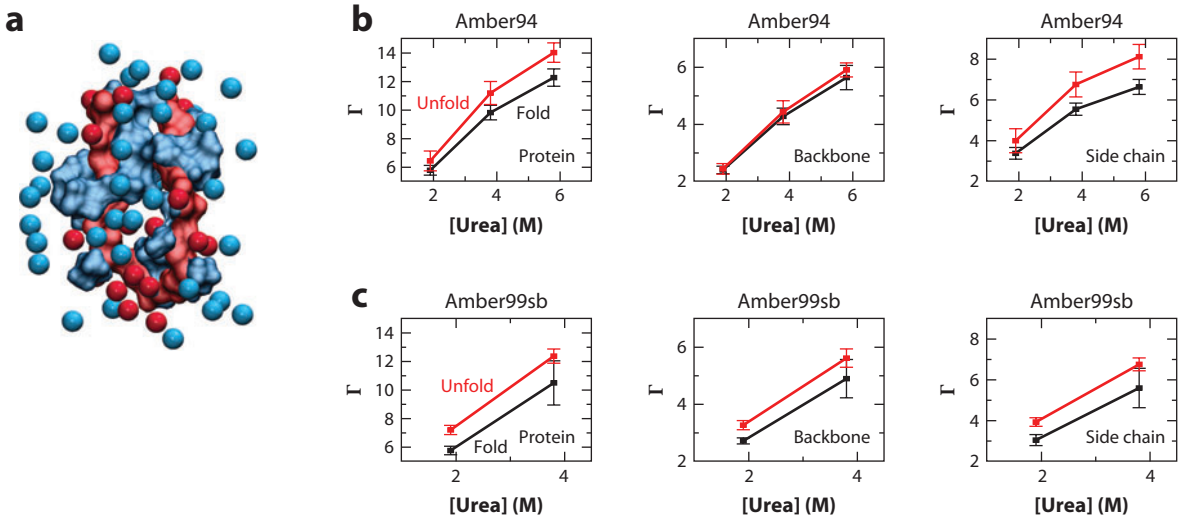

Figure 4

The preferential interaction of urea with Trp-cage (57). (*a*) Snapshot of Trp-cage interacting with urea. The protein backbone is colored in red, whereas the side chains are shown in blue. Urea molecules are shown as spheres, colored according to the group they are closest to. (*b*) The preferential interaction in the Amber94 model. The backbone does not make any contribution to the overall change in preferential interaction upon unfolding. (*c*) The preferential interaction in the Amber99sb model. The backbone and the side chains contribute approximately 40% and 60% to the overall change in preferential interaction upon unfolding, respectively. Figure adapted with permission from Reference 57. Copyright 2011, Elsevier.

for Trp-cage, with the rest accounted for by preferential interactions of the backbone and urea (**Figure 4*c***). This contrasts with predictions made from transfer model studies, in which the contribution of side chains has been found to be small or even unfavorable (35, 66).

Recent experimental studies of the interaction of urea with model compounds and amino acids support the scenario presented above. Lee et al. (37) measured the partial molar volumes and adiabatic compressibilities of the naturally occurring amino acids in urea solution, as a function of urea concentration. Using volumetric data in a binding model framework, they demonstrated that urea has favorable interactions with the backbone as well as most of the side-chain groups. Guinn et al. (38) took it further by measuring the interaction of urea with a wide range of model compounds, using osmometry to characterize its interaction with various types of molecular surfaces presented by the protein. Using the solute partitioning model, they reported urea accumulation in the vicinity of various groups presented by the protein in the following order:

amide O ∼ aromatic C > carboxyl O > amide N > hydroxyl O > aliphatic C.

The partition coefficient $K_p = \frac{m^{local}}{m^{bulk}}$, where m denotes the concentration, is the distribution of urea in local and bulk domains of the solute and ranges from 1.28 for amide O to 1.03 for aliphatic C. The interaction potentials derived from the above analysis were used to successfully predict the m-values for a wide range of proteins. The key realization in this work is that even though urea shows only a weak accumulation around the aliphatic C, this interaction contributes significantly to the observed effect of urea on protein stability because the composition of the surface exposed in unfolding is predominantly (∼65%) aliphatic C. The authors estimated a 55% contribution from the side chains to the m-value for the unfolding of the Trp-cage miniprotein, in good agreement with the values predicted from simulation studies (57).

One may ask why the transfer model studies predict a negligible contribution of the side chains to the free energy of unfolding (35, 66). The transfer free energies (δg^{tr}) for an amino acid are calculated from the difference in its solubility between urea and water solutions at the solubility limit. In the analysis of their data, Auton et al. (66) made nonideality corrections only for glycine and alanine but not for other amino acids. Guinn et al. (38) have suggested that the lack of nonideality correction leads to the discrepancy in δg^{tr} reported using solubility data and osmometry for many amino acids, which can lead to an erroneous contribution from the side chains to the unfolding free energy. Another possibility lies in the way the δg^{tr} of the side chain is calculated—by subtracting the δg^{tr} of glycine from the value for the entire amino acid. Comparing transfer free energies of two solutes directly to determine the δg^{tr} of a functional group does not account for their differing solubility limits, which can have a significant influence on the measured value (37).

Lim et al. (89) demonstrated that urea binds to the protein backbone by performing hydrogen exchange experiments on alanine dipeptide. Although in agreement with all the results described above, their data cannot be used to attribute the mechanism of urea denaturation to hydrogen bonding alone as they did not consider the interactions of side chains with urea.

Experimental and computational results now point toward the following mechanism for protein denaturation by urea. Urea is a small organic molecule, which is soluble in water in large concentrations and incorporates itself well in the hydrogen-bond network of water. It can accept and donate hydrogen bonds, while also presenting more sites for dispersion interaction than water by the virtue of its molecular structure. Urea accumulates in the vicinity of proteins owing to favorable direct interaction with them. The direct interaction is a result of the favorable interaction of urea with all protein moieties, including the peptide backbone and most of the side-chain groups to varying degrees (33, 34, 36–38, 56, 57). The unfolded ensemble has a larger preferential interaction with urea than the folded ensemble does, which provides an enthalpic driving force for unfolding. The hydrogen bonding of urea to the protein backbone is an important interaction in the process of denaturation, but it is not sufficient to entirely account for the destabilization of proteins in the presence of urea.

3. THE STABILIZATION OF PROTEINS BY TMAO

Protecting osmolytes are small organic molecules that stabilize the folded state of a protein. TMAO, a widely studied osmolyte, is found in many marine organisms that accumulate urea at elevated concentrations in their cells to counter osmotic stress (19). The presence of TMAO in these organisms counteracts the denaturing effect of urea of proteins, typically in a 2:1 concentration ratio of urea and TMAO, and thereby maintains cellular function. The mechanism by which TMAO stabilizes proteins and counteracts the effect of urea has been investigated, but the molecular details of these phenomena are still lacking.

Many interesting effects and applications of TMAO have been reported. Quite remarkably, TMAO can fold proteins that are thermodynamically unfolded to native-like structures with significant functional activity (90, 91). Based on this observation, investigators used urea-TMAO mixtures to measure the stability of partially folded proteins and reported that the *m*-value for urea denaturation was unaffected by the addition of TMAO (92). Calorimetric studies have indicated that the enthalpy of unfolding increases linearly with osmolyte concentration (93), suggesting that a direct interaction mechanism may be involved. The compensation of the opposite effects of TMAO and urea on the transition temperature, T_m, rather than the respective free energies has also been reported (94). TMAO has been observed to stabilize proteins against pressure denaturation, which is consistent with its occurrence in deep-sea animals (95). TMAO has also found application

in the design of protein-resistant surfaces (96), protein crystallography (97), and the prevention of misfolding diseases (98).

A wide variety of mechanisms has been proposed to explain the effects of TMAO on protein stability. An indirect mechanism has been suggested in which TMAO stabilizes proteins by enhancing water structure (99, 100). From dialysis and osmometry experiments, it is known that TMAO is preferentially excluded from protein surfaces (20, 94). Transfer free energies of amino acids from water to TMAO solutions have been used to suggest that the observed exclusion results from the osmophobic interaction of the peptide backbone with TMAO (101). In this model, the compensatory effect on protein stability in urea-TMAO solutions arises from the additivity of the favorable and unfavorable interactions of urea and TMAO, respectively, with the protein backbone. TMAO has also been shown to be strongly excluded from hydrophobic surfaces, suggesting that its exclusion from apolar side chains can contribute significantly to the increased protein stability (102). An entropic mechanism has been proposed in which TMAO acts as a crowding agent to favor the more compact native state of proteins through excluded volume effects (103). Neutron-scattering experiments have suggested that the compensatory effect of TMAO results from the direct interaction between TMAO and urea itself without the necessity of TMAO interacting with the protein directly, although this interaction was later shown to be weak (104, 105).

3.1. TMAO-Water Interactions

Recent experiments have studied the properties of aqueous TMAO solutions. Raman spectroscopy has indicated that TMAO forms hydrogen bonds with at least three water molecules and has suggested weak interactions of water with the methyl groups of TMAO (106). Femtosecond mid-infrared spectroscopy also suggested long-lived complexes (lifetime >50 ps) of TMAO with two or three water molecules (100). Using vibrational sum frequency spectroscopy, Sagle et al. (107) demonstrated that the methyl groups of TMAO orient away from hydrophobic interfaces. This is a significant finding that implies that not only does the oxide moiety have a tendency to be hydrated, but so do the methyl groups of TMAO, and this can cause a depletion of cosolvent molecules near protein surfaces. Koga et al. (108) reached a similar conclusion, showing that methyl groups need not always be hydophobic, especially when attached to a quaternary nitrogen. Rösgen & Jackson-Atogi (109) reported activity coefficient data for TMAO and urea-TMAO solutions, from which solvation properties have been derived using the KB theory. They showed that TMAO in water behaves effectively as hard spheres, and the binding of urea to TMAO is nearly random. These studies established that there is a strong interaction of TMAO with water, which must be considered in explaining the effects of TMAO on protein stability, whereas the lack of any strong favorable or unfavorable interaction between urea and TMAO may be the basis for the additivity of urea and TMAO effects.

3.2. Molecular Dynamics Simulation Studies

In contrast to the case of urea, relatively few MD simulation studies have addressed the effects of TMAO and urea-TMAO mixtures. Simulations of aqueous TMAO show that TMAO remains hydrated and does not tend to self-aggregate as its concentration is increased (110, 111). The scenario in which the strengthening of hydrophobic interactions in TMAO solutions leads to increased protein stability has not been supported by computational investigations. No effect on hydrophobic interactions was seen in TMAO solutions when compared to water, for small solutes as well as for the folding of a hydrophobic polymer (112). Disruption of the hydrophobic attraction between a neopentane pair by the addition of TMAO to both water and urea-water solutions has

been reported, implying that TMAO does not protect proteins against denaturation by enhancing the hydrophobic effect (113, 114). Polyglycine, a model for the peptide backbone, has been shown to collapse in TMAO solutions, and the exclusion of TMAO from the vicinity of the backbone was attributed to strong triplet correlations among the solute, TMAO, and water (115). Solvation free energy calculations of decalanine showed that the unfavorable transfer free energy to TMAO solutions from water arises from both the van der Waals and electrostatic components, unlike the case for urea in which the van der Waals component is favorable (116). The only simulation in the literature of a protein in urea-TMAO solutions was performed by Bennion & Daggett (117), who attributed the counteracting effect to an indirect mechanism, i.e., the ordering of the solvent by TMAO. Molecular simulation studies that can capture the effect of TMAO and urea-TMAO mixtures on the protein folding equilibrium, while making rigorous connections with experimental data (e.g., preferential interaction, *m*-value), can provide insight into the molecular underpinnings of these phenomena. Such studies will require the use of physically motivated force-field parameters for TMAO that address the balance of interactions in a multicomponent solution, similar to the KBFF model for urea (58). The development of such a model is addressed in the next section.

3.3. Simulating the Preferential Exclusion of TMAO from Proteins

Most molecular simulation studies of TMAO in the literature have employed the Kast model for TMAO (118), developed using ab initio methods. Canchi et al. (119) reported that the Kast model for TMAO does not show the expected preferential exclusion from protein surfaces and may even act as a denaturant. Extensive REMD simulations of the Trp-cage miniprotein in TMAO and 2:1 urea-TMAO systems did not show the stabilization of the protein expected due to the addition of TMAO (**Figure 5*a***). The authors conjectured that this behavior resulted from the inability of the Kast model to capture the thermodynamics of TMAO solutions. Using the Kast model as a starting point, they have developed a new model for TMAO by incorporating realistic water-TMAO interactions using osmotic pressure measurements of TMAO solutions, over a range of

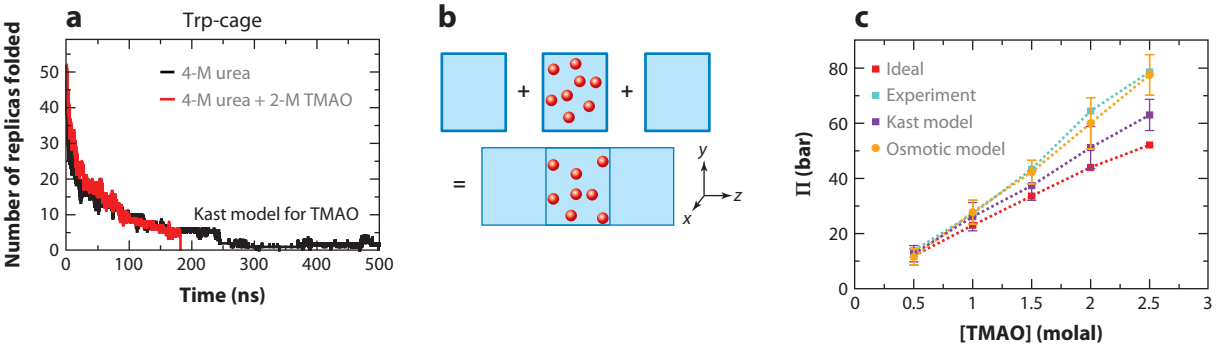

Figure 5

Model development for TMAO (119). (*a*) Replica exchange molecular dynamics simulations of Trp-cage in a 2:1 urea/TMAO mixture showing similar decay to equilibrium as in the simulation with urea alone, indicating that the Kast model is unable to capture the stabilization of proteins by TMAO. (*b*) Scheme to calculate osmotic pressure in molecular dynamics simulations. TMAO molecules (*red*) are confined to the central region, while water (*blue*) can diffuse freely. Osmotic pressure is obtained from the force required to confine TMAO to the central region. (*c*) The osmotic model for TMAO obtained by matching the osmotic pressure of TMAO from simulation to the experimental value, over a range of TMAO concentrations. Figure adapted with permission from Reference 119. Copyright 2012, American Chemical Society.

osmolyte concentration. The osmotic pressure, Π, for an ideal solution is given by the well-known van't Hoff law, i.e., $\Pi^{Ideal} = [C]RT$, where $[C]$ is the molar concentration of the solute. Deviation from ideality is accounted for using the osmotic coefficient, ϕ, defined as

Mixing rule: specifies the Lennard-Jones interaction among atoms of different types in an MD simulation

$$\phi = \frac{\Pi}{[C]RT} = \frac{\Pi_{Measured}}{\Pi_{Ideal}}. \quad (6)$$

A positive deviation from ideality ($\phi > 1$) implies solvent-mediated repulsive interactions between solute molecules, whereas a negative deviation from ideality ($\phi < 1$) indicates a net attractive interaction among solute molecules. The osmotic pressure can be calculated directly from MD simulations using the scheme shown in **Figure 5*b*** (120). An equilibrated solution of a given osmolyte concentration is assembled with systems of solvent (water) of identical size. The resulting system is simulated by applying a spatial confining potential only on solute particles to restrain them to occupy their original volume, while solvent molecules are free to diffuse throughout the system. The confining potential acts as a semipermeable membrane, whereas freely diffusing water mimics the constant solvent chemical potential. The osmotic pressure is then calculated from the average force required to confine the solutes to their original volume during the simulation.

Figure 5*c* shows that the measured osmotic pressure for TMAO solutions is larger than the ideal value ($\phi > 1$), implying a net repulsive interaction between TMAO molecules in solution (i.e., a strong TMAO-water interaction). The osmotic pressure calculated for TMAO using the Kast model shows a net repulsive interaction as the TMAO concentration increases, although not to the extent suggested by experiments at larger concentrations. A new model for TMAO was obtained that increased the net repulsion among TMAO molecules to match experiments, termed the osmotic model, by making two changes to the Kast model: (*a*) scale up the charges to strengthen the interaction of TMAO with water and (*b*) weaken the LJ interaction among TMAO molecules by using a nondefault mixing rule. The osmotic model for TMAO displayed greater preferential exclusion from protein surfaces than the Kast model for a range of model systems and proteins, as a consequence of using the osmotic data to capture the thermodynamics of TMAO-water mixtures (**Figure 6*a***). The interaction of TMAO with proteins can be determined using further experimental inputs, such as the *m*-value for protein unfolding in TMAO, or by measuring the change in osmotic pressure resulting from the addition of the protein to the TMAO-water solution (119).

Furthermore, Canchi et al. (119) examined the role of interaction among cosolvent molecules, as manifested by the osmotic pressure, in determining its preferential interaction with proteins (**Figure 6*b***). They studied the osmotic pressure as a function of the polarity of TMAO by scaling the charges on the reference Kast model. Scaling by a factor $\alpha > 1$ makes the molecule more hydrophilic and increases the osmotic pressure of the TMAO-water solution, whereas the opposite holds true for $\alpha < 1$. The preferential interaction of TMAO with the protein surface, shown for Trp-cage in **Figure 6*b***, varies concomitantly with the polarity (or the osmotic pressure) of TMAO. Making TMAO molecules more attractive leads to an increase in the preferential interaction with the protein, whereas increasing the solvent-mediated repulsion leads to greater preferential exclusion from the protein's vicinity. Qualitatively similar behavior for the preferential interaction was observed in such simulations with urea.

The intimate connection between preferential exclusion and osmotic pressure provides physical insight into the role of solute-solute interaction in determining the preferential accumulation or exclusion of cosolvents from proteins. Denaturants, such as urea, have weak favorable interactions with protein surfaces, and a significant concentration of cosolvent is required to denature the proteins. In addition to favorable interactions with proteins, denaturants must also be

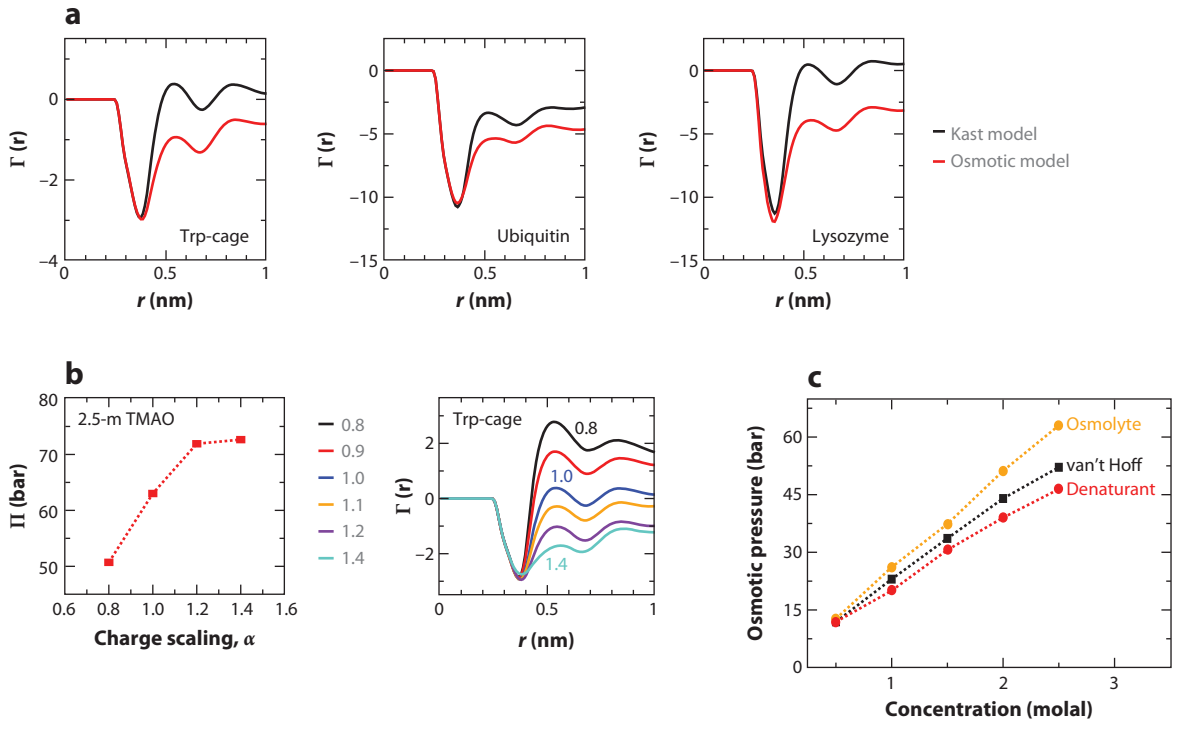

Figure 6

Osmotic pressure and preferential interaction. (*a*) The osmotic model for TMAO, showing greater exclusion from protein surfaces than the Kast model, as a consequence of the osmotic pressure parameterization. (*b*) The osmotic pressure of the TMAO solution, which can be controlled in simulations by uniformly scaling the charge on the reference Kast model ($\alpha = 1$). The preferential interaction of TMAO with Trp-cage responds concomitantly to the osmotic pressure of the TMAO solution. (*c*) The osmotic behavior of cosolvents. It is hypothesized that osmolytes (*orange*) show a positive deviation from the van't Hoff law (*black*), whereas denaturants (*red*) show a negative deviation. Figure adapted with permission from Reference 119. Copyright 2012, American Chemical Society.

able to admit their own excess concentrations in the vicinity (local domain) of the protein, i.e., show a negative deviation from ideality with the osmotic coefficient $\phi \leq 1$. Solvent-mediated repulsion among osmolyte molecules ($\phi > 1$), apart from the repulsive interaction with protein moieties, adds another penalty that makes the accumulation of osmolytes in the vicinity of the protein unfavorable. Canchi et al. suggest that denaturants and osmolytes lie on opposite sides of the ideal osmotic pressure curve given by the van't Hoff law (**Figure 6*c***). From experimental osmotic pressure data, this scenario is true for urea and TMAO, as well as for other osmolytes, such as betaine, trehalose, proline, and glycerol (20). By this principle, a mixture of two protecting osmolytes that have repulsive interactions among themselves as reflected by the nonadditivity of their osmotic pressure may show a synergistic enhancement of protein stability.

The TMAO model of Canchi et al., obtained by scaling the ab initio charges of the Kast model (118), represents only one possible parameterization for the molecule. Another approach based on modifying the LJ parameters of the Kast model also reproduces the osmotic data (R.R. Netz, personal communication). The robustness of the mechanism of protein stabilization by TMAO provided by these models is still to be determined.

CONCLUSIONS

The control of protein stability by the addition of cosolvents is a biophysical problem of great fundamental interest, with many practical applications in biotechnology. Understanding the molecular mechanism of these phenomena has attracted much interest in the literature. The mechanism by which urea denatures proteins has been a contentious issue, but recent computational and experimental studies point toward an emerging consensus. Urea accumulates in the vicinity of the protein owing to favorable direct interactions with the protein backbone as well as a range of amino acid side chains. More favorable protein-urea interactions can be formed in the unfolded ensemble than in the folded ensemble, which provides an enthalpic driving force for unfolding.

The stabilization of proteins by TMAO and its counteraction of destabilization by urea have not been satisfactorily explained. Recent studies have shown that the strong interaction of TMAO with water plays an important role in determining its preferential exclusion from protein surfaces. Thermodynamic measurements that characterize the interactions of TMAO with amino acids and model compounds, along with molecular simulations that can capture the effect of TMAO on the protein folding equilibrium, have the potential to provide insights into the mechanism of these intriguing phenomena.

DISCLOSURE STATEMENT

The authors are not aware of any affiliations, memberships, funding, or financial holdings that might be perceived as affecting the objectivity of this review.

ACKNOWLEDGMENTS

This work has been funded by the National Science Foundation (NSF MCB-1050966) and the National Institutes of Health (GM086801). We thank M.T. Record, G.I. Makhatadze, D. Thirumalai, D. Rao, and D. Paschek for advice, comments, and suggestions.

LITERATURE CITED

1. Anfinsen CB. 1973. Principles that govern folding of protein chains. *Science* 181:223–30
2. Bryngelson JD, Onuchic JN, Socci ND, Wolynes PG. 1995. Funnels, pathways, and the energy landscape of protein folding: a synthesis. *Proteins* 21:167–95
3. Onuchic JN, Luthey-Schulten Z, Wolynes PG. 1997. Theory of protein folding: the energy landscape perspective. *Annu. Rev. Phys. Chem.* 48:545–600
4. Makhatadze GI, Privalov PL. 1995. Energetics of protein structure. *Adv. Protein Chem.* 47:307–425
5. Privalov PL. 1990. Cold denaturation of proteins. *Crit. Rev. Biochem. Mol. Biol.* 25:281–305
6. Heremans K. 1982. High-pressure effects on proteins and other biomolecules. *Annu. Rev. Biophys. Bioeng.* 11:1–21
7. Timasheff SN. 1993. The control of protein stability and association by weak interactions with water: How do solvents affect these processes? *Annu. Rev. Biophys. Biomol. Struct.* 22:67–97
8. Kauzmann W. 1987. Protein stabilization: thermodynamics of unfolding. *Nature* 325:763–64
9. Silva JL, Foguel D, Royer CA. 2001. Pressure provides new insights into protein folding, dynamics and structure. *Trends Biochem. Sci.* 26:612–18
10. Royer CA. 2002. Revisiting volume changes in pressure-induced protein unfolding. *Biochim. Biophys. Acta* 1595:201–9
11. Hummer G, Garde S, García AE, Paulaitis ME, Pratt LR. 1998. The pressure dependence of hydrophobic interactions is consistent with the observed pressure denaturation of proteins. *Proc. Natl. Acad. Sci. USA* 95:1552–55

12. Sarupria S, Ghosh T, García AE, Garde S. 2010. Studying pressure denaturation of a protein by molecular dynamics simulations. *Proteins* 78:1641–51
13. Roche J, Caro JA, Norberto DR, Barthe P, Roumestand C, et al. 2012. Cavities determine the pressure unfolding of proteins. *Proc. Natl. Acad. Sci. USA* 109:6945–50
14. Brandts JF, Oliveira RJ, Westort C. 1970. Thermodynamics of protein denaturation: effect of pressure on denaturation of ribonuclease A. *Biochemistry* 9:1038–47
15. Hawley SA. 1971. Reversible pressure-temperature denaturation of chymotrypsinogen. *Biochemistry* 10:2436–42
16. Paschek D, Gnanakaran S, García AE. 2005. Simulations of the pressure and temperature unfolding of an α-helical peptide. *Proc. Natl. Acad. Sci. USA* 102:6765–70
17. Paschek D, Hempel S, García AE. 2008. Computing the stability diagram of the Trp-cage miniprotein. *Proc. Natl. Acad. Sci. USA* 105:17754–59
18. Day R, Paschek D, García AE. 2010. Microsecond simulations of the folding/unfolding thermodynamics of the Trp-cage miniprotein. *Proteins* 78:1889–99
19. Yancey PH, Clark ME, Hand SC, Bowlus RD, Somero GN. 1982. Living with water stress: evolution of osmolyte systems. *Science* 217:1214–22
20. Courtenay ES, Capp MW, Anderson CF, Record MT. 2000. Vapor pressure osmometry studies of osmolyte-protein interactions: implications for the action of osmoprotectants in vivo and for the interpretation of "osmotic stress" experiments in vitro. *Biochemistry* 39:4455–71
21. Bolen DW, Rose G. 2008. Structure and energetics of the hydrogen-bonded backbone in protein folding. *Annu. Rev. Biochem.* 77:339–62
22. Wang A, Bolen DW. 1997. A naturally occuring protective system in urea-rich cells: mechanism of osmolyte protection of proteins against urea denaturation. *Biochemistry* 36:9101–8
23. Kauzmann W. 1959. Some factors in the interpretation of protein denaturation. *Adv. Protein Chem.* 14:1–63
24. Pace C. 1986. Determination and analysis of urea and guanidine hydrochloride denaturation curves. *Methods Enzymol.* 131:266–80
25. Makhatadze GI. 1999. Thermodynamics of protein interactions with urea and guanidinium chloride. *J. Phys. Chem. B* 103:4781–85
26. Frank HS, Franks F. 1968. Structural approach to solvent power of water for hydrocarbons: urea as a structure breaker. *J. Chem. Phys.* 48:4746–57
27. Dill KA. 1990. Dominant forces in protein folding. *Biochemistry* 29:7133–55
28. Soper AK, Castner EW, Luzar A. 2003. Impact of urea on water structure: a clue to its properties as a denaturant? *Biophys. Chem.* 105:649–66
29. Batchelor JD, Olteanu A, Tripathy A, Pielak GJ. 2004. Impact of protein denaturants and stabilizers on water structure. *J. Am. Chem. Soc.* 126:1958–61
30. Rezus YLA, Bakker HJ. 2006. Effect of urea on the structural dynamics of water. *Proc. Natl. Acad. Sci. USA* 103:18417–20
31. Kokubo H, Pettitt BM. 2007. Preferential solvation in urea solutions at different concentrations: properties from simulation studies. *J. Phys. Chem. B* 111:5233–42
32. Stumpe MC, Grubmuller H. 2007. Aqueous urea solutions: structure, energetics, and urea aggregation. *J. Phys. Chem. B* 111:6220–28
33. Hua L, Zhou RH, Thirumalai D, Berne BJ. 2008. Urea denaturation by stronger dispersion interactions with proteins than water implies a two-stage unfolding. *Proc. Natl. Acad. Sci. USA* 105:16928–33
34. Horinek D, Netz RR. 2011. Can simulations quantitatively predict peptide transfer free energies to urea solutions? Thermodynamic concepts and force field limitations. *J. Phys. Chem. A* 115:6125–36.
35. Auton M, Bolen DW. 2005. Predicting the energetics of osmolyte-induced protein folding/unfolding. *Proc. Natl. Acad. Sci. USA* 102:15065–68
36. Stumpe MC, Grubmuller H. 2007. Interaction of urea with amino acids: implications for urea-induced protein denaturation. *J. Am. Chem. Soc.* 129:16126–31
37. Lee S, Shek YL, Chalikian TV. 2010. Urea interactions with protein groups: a volumetric study. *Biopolymers* 93:866–79

21. Reviews the understanding of cosolvent-dependent protein stability based on transfer model studies.

34. Presents a thermodynamic analysis that separates the direct and indirect effects of urea in MD simulations.

37. Presents volumetric measurements of the interaction of urea with amino acids.

38. Guinn EJ, Pegram LM, Capp MW, Pollock MN, Record MT. 2011. Quantifying why urea is a protein denaturant, whereas glycine betaine is a protein stabilizer. *Proc. Natl. Acad. Sci. USA* 108:16932–37

38. Quantifies the interaction of urea with various types of molecular surfaces presented by a protein by osmometry.

39. Rossky PJ. 2008. Protein denaturation by urea: slash and bond. *Proc. Natl. Acad. Sci. USA* 105:16825–26
40. Wallqvist A, Covell DG, Thirumalai D. 1998. Hydrophobic interactions in aqueous urea solutions with implications for the mechanism of protein denaturation. *J. Am. Chem. Soc.* 120:427–28
41. Shimizu S, Chan HS. 2002. Origins of protein denatured state compactness and hydrophobic clustering in aqueous urea: inferences from nonpolar potentials of mean force. *Proteins Struct. Funct. Genet.* 49:560–66
42. Oostenbrink C, van Gunsteren WF. 2005. Methane clustering in explicit water: effect of urea on hydrophobic interactions. *Phys. Chem. Chem. Phys.* 7:53–58
43. Lee ME, van der Vegt NFA. 2006. Does urea denature hydrophobic interactions? *J. Am. Chem. Soc.* 128:4948–49
44. O'Brien EP, Dima RI, Brooks B, Thirumalai D. 2007. Interactions between hydrophobic and ionic solutes in aqueous guanidinium chloride and urea solutions: lessons for protein denaturation mechanism. *J. Am. Chem. Soc.* 129:7346–53
45. England JL, Pande VS, Haran G. 2008. Chemical denaturants inhibit the onset of dewetting. *J. Am. Chem. Soc.* 130:11854–55
46. Zangi R, Zhou RH, Berne BJ. 2009. Urea's action on hydrophobic interactions. *J. Am. Chem. Soc.* 131:1535–41
47. Yang LJ, Gao YQ. 2010. Effects of cosolvents on the hydration of carbon nanotubes. *J. Am. Chem. Soc.* 132:842–48
48. Das P, Zhou RH. 2010. Urea-induced drying of carbon nanotubes suggests existence of a dry globule-like transient state during chemical denaturation of proteins. *J. Phys. Chem. B* 114:5427–30
49. Tirado-Rives J, Orozco M, Jorgensen WL. 1997. Molecular dynamics simulations of the unfolding of barnase in water and 8 m aqueous urea. *Biochemistry* 36:7313–29
50. Bennion BJ, Daggett V. 2003. The molecular basis for the chemical denaturation of proteins by urea. *Proc. Natl. Acad. Sci. USA* 100:5142–47
51. Caballero-Herrera A, Nordstrand K, Berndt KD, Nilsson L. 2005. Effect of urea on peptide conformation in water: molecular dynamics and experimental characterization. *Biophys. J.* 89:842–57
52. Stumpe MC, Grubmuller H. 2008. Polar or apolar: the role of polarity for urea-induced protein denaturation. *PLoS Comput. Biol.* 4:e1000221
53. Smith LJ, Jones RM, van Gunsteren WF. 2005. Characterization of the denaturation of human α-lactalbumin in urea by molecular dynamics simulations. *Proteins Struct. Funct. Genet.* 58:439–49
54. Tobi D, Elber R, Thirumalai D. 2003. The dominant interaction between peptide and urea is electrostatic in nature: a molecular dynamics simulation study. *Biopolymers* 68:359–69
55. Klimov DK, Straub JE, Thirumalai D. 2004. Aqueous urea solution destabilizes amyloid β(16–22) oligomers. *Proc. Natl. Acad. Sci. USA* 101:14760–65

56. Canchi DR, Paschek D, García A. 2010. Equilibrium study of protein denaturation by urea. *J. Am. Chem. Soc.* 132:2338–44

56. Presents an REMD simulation of the folding equilibrium of the Trp-cage miniprotein in urea.

57. Canchi DR, García AE. 2011. Backbone and side-chain contributions in protein denaturation by urea. *Biophys. J.* 100:1526–33

57. Addresses the contribution of backbone and side-chain interaction with urea to the unfolding free energy of Trp-cage, based on preferential interaction analysis of REMD data.

58. Weerasinghe S, Smith PE. 2003. A Kirkwood-Buff derived force field for mixtures of urea and water. *J. Phys. Chem. B* 107:3891–98

58. Gives a molecular model for urea consistent with the thermodynamics of aqueous urea.

59. Weerasinghe S, Smith PE. 2003. A Kirkwood-Buff derived force field for sodium chloride in water. *J. Chem. Phys.* 119:11342–49
60. Weerasinghe S, Smith PE. 2004. A Kirkwood-Buff derived force field for the simulation of aqueous guanidinium chloride solutions. *J. Chem. Phys.* 121:2180–86
61. Weerasinghe S, Smith PE. 2005. A Kirkwood-Buff derived force field for methanol and aqueous methanol solutions. *J. Phys. Chem. B* 109:15080–86
62. Kirkwood JG, Buff FP. 1951. The statistical mechanical theory of solutions. 1. *J. Chem. Phys.* 19:774–77
63. Ben-Naim A. 2006. *Molecular Theory of Solutions*. New York: Oxford Univ. Press

64. Duffy E, Severance D, Jorgenson W. 1993. Urea: potential functions, log p, and free energy of hydration. *Isr. J. Chem.* 33:323
65. Tanford C. 2004. Isothermal unfolding of globular proteins in aqueous urea solutions. *J. Am. Chem. Soc.* 126:1958–61
66. Auton M, Holthauzen LMF, Bolen DW. 2007. Anatomy of energetic changes accompanying urea-induced protein denaturation. *Proc. Natl. Acad. Sci. USA* 104:15317–22
67. Merchant KA, Best RB, Louis JM, Gopich IV, Eaton WA. 2007. Characterizing the unfolded states of proteins using single-molecule FRET spectroscopy and molecular simulations. *Proc. Natl. Acad. Sci. USA* 104:1528–33
68. O'Brien EP, Ziv G, Haran G, Brooks BR, Thirumalai D. 2008. Effects of denaturants and osmolytes on proteins are accurately predicted by the molecular transfer model. *Proc. Natl. Acad. Sci. USA* 105:13403–8
69. Berteotti A, Barducci A, Parrinello M. 2011. Effect of urea on the β-hairpin conformational ensemble and protein denaturation mechanism. *J. Am. Chem. Soc.* 133:17200–6
70. Ziv G, Haran G. 2009. Protein folding, protein collapse, and Tanford's transfer model: lessons from single-molecule FRET. *J. Am. Chem. Soc.* 131:2942–47
71. England JL, Haran G. 2011. Role of solvation effects in protein denaturation: from thermodynamics to single molecules and back. *Annu. Rev. Phys. Chem.* 62:257–77
72. Yoo TY, Meisburger SP, Hinshaw J, Pollack L, Haran G, et al. 2012. Small-angle X-ray scattering and single-molecule FRET spectroscopy produce highly divergent views of the low-denaturant unfolded state. *J. Mol. Biol.* 418:226–36
73. Timasheff SN. 2002. Protein-solvent preferential interactions, protein hydration, and the modulation of biochemical reactions by solvent components. *Proc. Natl. Acad. Sci. USA* 99:9721–26
74. Arakawa T, Timasheff SN. 1982. Preferential interactions of proteins with salts in concentrated solutions. *Biochemistry* 21:6545–52
75. Record MT, Anderson CF. 1995. Interpretation of preferential interaction coefficients of nonelectrolytes and of electrolyte ions in terms of a two-domain model. *Biophys. J.* 68:786–94
76. Parsegian VA, Rand RP, Rau DC. 2000. Osmotic stress, crowding, preferential hydration and binding: a comparison of perspectives. *Proc. Natl. Acad. Sci. USA* 97:3987–92
77. Shukla D, Shinde C, Trout BL. 2009. Molecular computations of preferential interaction coefficients of proteins. *J. Phys. Chem. B* 113:12546–54
78. Neidigh JW, Fesinmeyer RM, Andersen NH. 2002. Designing a 20-residue protein. *Nat. Struct. Biol.* 9:425–30
79. Qiu LL, Pabit SA, Roitberg AE, Hagen SJ. 2002. Smaller and faster: the 20-residue Trp-cage protein folds in 4 μs. *J. Am. Chem. Soc.* 124:12952–53
80. Ahmed Z, Beta IA, Mikhonin AV, Asher SA. 2005. UV-resonance Raman thermal unfolding study of Trp-cage shows that it is not a simple two-state miniprotein. *J. Am. Chem. Soc.* 127:10943–50
81. Neuweiler H, Doose S, Sauer M. 2005. A microscopic view of miniprotein folding: enhanced folding efficiency through formation of an intermediate. *Proc. Natl. Acad. Sci. USA* 102:16650–55
82. Wafer LNR, Streicher WW, Makhatadze GI. 2010. Thermodynamics of the Trp-cage miniprotein unfolding in urea. *Proteins* 78:1376–81
83. Streicher WW, Makhatadze GI. 2007. Unfolding thermodynamics of Trp-cage, a 20 residue miniprotein, studied by differential scanning calorimetry and circular dichroism spectroscopy. *Biochemistry* 46:2876–80
84. Cornell WD, Cieplak P, Bayly CI, Gould IR, Merz KM Jr, et al. 1995. A second generation force field for the simulation of proteins, nucleic acids, and organic molecules. *J. Am. Chem. Soc.* 117:5179–97
85. Hornak V, Abel R, Okur A, Strockbine B, Roitberg A, Simmerling C. 2006. Comparison of multiple amber force fields and development of improved protein backbone parameters. *Proteins* 65:712–25
86. Jorgensen WL, Chandrasekhar J, Madura JD, Impey RW, Klein ML. 1983. Comparison of simple potential functions for simulating liquid water. *J. Chem. Phys.* 79:926–35
87. Myers JK, Pace CN, Scholtz JM. 1995. Denaturant m-values and heat-capacity changes: relation to changes in accessible surface areas of protein unfolding. *Protein Sci.* 4:2138–48
88. Mehrotra PK, Beveridge DL. 1980. Structural analysis of molecular solutions based on quasi-component distribution functions: application to $[H_2CO]_{aq}$ at 25°C. *J. Am. Chem. Soc.* 102:4287–94

70. Presents a theoretical analysis that shows that denaturants modulate the collapse transition of proteins.

89. Lim WK, Rösgen J, Englander SW. 2009. Urea, but not guanidinium, destabilizes proteins by forming hydrogen bonds to the peptide group. *Proc. Natl. Acad. Sci. USA* 106:2595–600
90. Baskakov I, Bolen DW. 1998. Forcing thermodynamically unfolded proteins to fold. *J. Biol. Chem.* 273:4831–34
91. Qu YX, Bolen CL, Bolen DW. 1998. Osmolyte-driven contraction of a random coil protein. *Proc. Natl. Acad. Sci. USA* 95:9268–73
92. Mello CC, Barrick D. 2003. Measuring the stability of partly folded proteins using TMAO. *Protein Sci.* 12:1522–29
93. Attri P, Venkatesu P, Lee MJ. 2010. Influence of osmolytes and denaturants on the structure and enzyme activity of α-chymotrypsin. *J. Phys. Chem. B* 114:1471–78
94. Lin TY, Timasheff SN. 1994. Why do some organisms use a urea-methylamine mixture as osmolyte? Thermodynamic compensation of urea and trimethylamine *N*-oxide interactions with protein. *Biochemistry* 33:12695–701
95. Krywka C, Sternemann C, Paulus M, Tolan M, Royer C, Winter R. 2008. Effect of osmolytes on pressure-induced unfolding of proteins: a high-pressure SAXS study. *ChemPhysChem* 9:2809–15
96. Anand G, Jamadagni SN, Garde S, Belfort G. 2010. Self-assembly of TMAO at hydrophobic interfaces and its effect on protein adsorption: insights from experiments and simulations. *Langmuir* 26:9695–702
97. Mueller-Dieckmann C, Kauffman B, Weiss M. 2011. Trimethylamine *N*-oxide as a versatile cryoprotective agent in macromolecular crystallography. *J. Appl. Crystallogr.* 44:433–36
98. Borwankar T, Röthlein C, Zhang G, Techen A, Dosche C, Ignatova Z. 2011. Natural osmolytes remodel the aggregation pathway of mutant huntingtin exon 1. *Biochemistry* 50:2048–60
99. Zou Q, Bennion BJ, Daggett V, Murphy KP. 2002. The molecular mechanism of stabilization of proteins by TMAO and its ability to counteract the effects of urea. *J. Am. Chem. Soc.* 124:1192–202
100. Hunger J, Tielrooij KJ, Buchner R, Bonn M, Bakker HJ. 2012. Complex formation in aqueous trimethylamine-*N*-oxide (TMAO) solutions. *J. Phys. Chem. B* 116:4783–95
101. Bolen DW, Baskakov IV. 2001. The osmophobic effect: natural selection of a thermodynamic force in protein folding. *J. Mol. Biol.* 310:955–63
102. Stanley C, Rau DC. 2008. Assessing the interaction of urea and protein stabilizing osmolytes with the nonpolar surface of hydroxypropylcellulose. *Biochemistry* 47:6711–18
103. Cho SS, Reddy G, Straub JE, Thirumalai D. 2011. Entropic stabilization of proteins by TMAO. *J. Phys. Chem. B* 115:13401–7
104. Meersman F, Bowron D, Soper AK, Koch MHJ. 2009. Counteraction of urea by trimethylamine *N*-oxide is due to direct interaction. *Biophys. J.* 97:2559–66
105. Meersman F, Bowron D, Soper AK, Koch MHJ. 2011. An X-ray and neutron scattering study of the equilibrium between trimethylamine *N*-oxide and urea in aqueous solution. *Phys. Chem. Chem. Phys.* 13:13765–71

107. Demonstrates a VSFS study of TMAO orientation near hydrophobic surfaces.

106. Munroe KL, Magers DH, Hammer NI. 2011. Raman spectroscopic signatures of noncovalent interactions between trimethylamine *N*-oxide (TMAO) and water. *J. Phys. Chem. B* 115:7699–707
107. Sagle LB, Cimatu K, Litosh VA, Liu Y, Flores SC, et al. 2011. Methyl groups of trimethylamine *N*-oxide orient away from hydrophobic interfaces. *J. Am. Chem. Soc.* 133:18707–12
108. Koga Y, Westh P, Nishikawa K, Subramanian S. 2011. Is a methyl group always hydrophobic? Hydrophilicity of trimethylamine-*N*-oxide, tetramethyl urea and tetramethylammonium ion. *J. Phys. Chem. B* 115:2995–3002

109. Presents thermodynamic data for TMAO and urea-TMAO solutions.

109. Rösgen J, Jackson-Atogi R. 2012. Volume exclusion and H-bonding dominate the thermodynamics and solvation of trimethylamine-*N*-oxide in aqueous urea. *J. Am. Chem. Soc.* 134:3590–97
110. Fornili A, Civera M, Sironi M, Fornili SL. 2003. Molecular dynamics simulation of aqueous solutions of trimethylamine-*N*-oxide and tert-butyl alcohol. *Phys. Chem. Chem. Phys.* 5:4905–10
111. Sinibaldi R, Casieri C, Melchionna S, Onori G, Segre AL, et al. 2006. The role of water coordination in binary mixtures: a study of two model amphiphilic molecules in aqueous solutions by molecular dynamics and NMR. *J. Phys. Chem. B* 110:8885–92

112. Examines the effect of TMAO on hydrophobic interactions.

112. Athawale MV, Dordick JS, Garde S. 2005. Osmolyte trimethylamine-*N*-oxide does not affect the strength of hydrophobic interactions: origin of osmolyte compatibility. *Biophys. J.* 89:858–66

113. Paul S, Patey GN. 2007. The influence of urea and trimethylamine-*N*-oxide on hydrophobic interactions. *J. Phys. Chem. B* 111:7932–33
114. Paul S, Patey GN. 2008. Hydrophobic interactions in urea: trimethylamine-*N*-oxide solutions. *J. Phys. Chem. B* 112:11106–11
115. Hu CY, Lynch GC, Kokubo H, Pettitt BM. 2010. Trimethylamine *N*-oxide influence on the backbone of proteins: an oligoglycine model. *Proteins* 78:695–704
116. Kokubo H, Hu CY, Pettitt BM. 2011. Peptide conformational preferences in osmolyte solutions: transfer free energies of decaalanine. *J. Am. Chem. Soc.* 133:1849–58
117. Bennion BJ, Daggett V. 2004. Counteraction of urea-induced protein denaturation by trimethylamine *N*-oxide: a chemical chaperone at atomic resolution. *Proc. Natl. Acad. Sci. USA* 101:6433–38
118. Kast KM, Brickmann J, Kast SM, Berry RS. 2003. Binary phases of aliphatic *N*-oxides and water: force field development and molecular dynamics simulation. *J. Phys. Chem. A* 107:5342–51
119. Canchi DR, Jayasimha P, Rau DC, Makhatadze GI, Garcia AE. 2012. Molecular mechanism for the preferential exclusion of TMAO from protein surfaces. *J. Phys. Chem. B* 116:12095–104
120. Luo Y, Roux B. 2010. Simulation of osmotic pressure in concentrated aqueous salt solutions. *J. Phys. Chem. Lett.* 1:183–89

119. Proposes a molecular model for TMAO based on osmotic data.

Annual Review of
Physical Chemistry
Volume 64, 2013

Contents

Indexes

Errata

An online log of corrections to *Annual Review of Physical Chemistry* articles may be found at http://physchem.annualreviews.org/errata.shtml